JBC Papers in Press. Published on January 25, 2013 as Manuscript M112.441535
The latest version is at http://www.jbc.org/cgi/doi/10.1074/jbc.M112.441535

Nuclear envelope composition determines the ability of neutrophil-type cells to passage through micron-scale constrictions

Amy C. Rowat[1,2,5], Diana E. Jaalouk[2,3], Monika Zwerger[2,4], W. Lloyd Ung[5], Irwin A. Eydelnant[5], Don E. Olins[6], Ada L. Olins[6], Harald Herrmann[7], David A. Weitz[5], Jan Lammerding[2,8]

[1]From the Department of Integrative Biology and Physiology, University of California, Los Angeles, Terasaki Life Sciences Building 1125, 610 Charles E. Young Dr. South, Los Angeles, CA 90095
[2]Department of Medicine, Brigham and Women's Hospital/Harvard Medical School, Cambridge, MA 02139
[3]Current Address: Department of Biology, American University of Beirut, Lebanon
[4]Current Address: Department of Biochemistry, University of Zurich, Switzerland
[5]Department of Physics and School of Engineering and Applied Sciences, Harvard University, Cambridge, MA 02138
[6]Department of Pharmaceutical Sciences, College of Pharmacy, University of New England, Portland, ME 04103
[7]Division of Molecular Genetics, German Cancer Research Center, D-69120 Heidelberg, Germany
[8]Weill Institute for Cell and Molecular Biology, Department of Biomedical Engineering, Cornell University, Ithaca, NY 14853

*Running Title: Physical properties of the neutrophil nucleus

To whom correspondence should be addressed:
Amy C. Rowat, Department of Integrative Biology and Physiology; Terasaki Life Sciences Building, 1125; 610 Charles E. Young Drive South; Los Angeles, CA 90095 USA; Phone: +1-310-825-4026; Fax: +1-310-206-9184; Email: rowat@ucla.edu

Keywords: Cell mechanics; granulopoiesis; HL60

Background: The unusual nuclear shape of neutrophils has been speculated to facilitate their passage through confined spaces.
Results: Levels of nuclear protein lamin A modulate cell passage through micron-scale pores.
Conclusion: The unique protein composition of neutrophil nuclei facilitates their deformation; lobulated nuclear shape is not essential.
Significance: Altered nuclear envelope composition, as reported in cancer cells, could impact cell passage through physiological gaps.

SUMMARY

Neutrophils are characterized by their distinct nuclear shape, which is thought to facilitate the transit of these cells through pore spaces less than one-fifth of their diameter. We used human promyelocytic leukemia (HL-60) cells as a model system to investigate the effect of nuclear shape in whole cell deformability. We probed neutrophil-differentiated HL-60 cells lacking expression of lamin B receptor (LBR), which fail to develop lobulated nuclei during granulopoiesis and present an *in vitro* model for Pelger-Huët anomaly; despite the circular morphology

of their nuclei, the cells passed through micron-scale constrictions on similar timescales as scrambled controls. We then investigated the unique nuclear envelope composition of neutrophil-differentiated HL-60 cells, which may also impact their deformability: while lamin A is typically downregulated during granulopoiesis, we genetically modified HL-60 cells to generate a subpopulation of cells with well-defined levels of ectopic lamin A. The lamin A-overexpressing neutrophil-type cells showed similar functional characteristics as the mock controls, but they had an impaired ability to pass through micron-scale constrictions. Our results suggest that levels of lamin A have a marked effect on the ability of neutrophils to passage through micron-scale constrictions, whereas the unusual multi-lobed shape of the neutrophil nucleus is less essential.

The passage of cells through narrow spaces is critical in physiological and disease processes from immune response to metastasis. For example, neutrophils are required to rapidly traverse constrictions that are much smaller than their own diameter of 7 – 8 μm: during perfusion through capillaries with diameters as small as 2 μm or during migration through transendothelial and interstitial spaces ranging from 0.1 to 10 μm (1). The ability of neutrophils to transit through narrow constrictions is essential; increased cell stiffness results in retention of neutrophils in arteries and capillaries (2), as well as accumulation in postcapillary venules leading to inflammation in the vascular bed (3).

While the mechanical properties of neutrophils can be regulated by cytoskeletal filaments such as actin (4-6) and microtubules (7), the hallmark multi-lobed nuclear morphology has long been thought to facilitate the deformation of neutrophils through narrow spaces (8,9): a round-shaped nucleus could sterically hinder the deformation of a cell through a narrow pore, while the multi-lobed neutrophil nucleus could aid cell passage, as individual lobes could be sequentially 'threaded' through constrictions. Indeed, cells with lobulated nuclear shape show less retention in 8 μm-porous membranes compared to their progenitors with round nuclei (10). However, it remains unclear to what extent this hyperlobulated nuclear shape is required for neutrophils to deform through narrow gaps: tightly regulated modifications in nuclear envelope protein composition also occur during granulopoiesis. Specifically, during the process of granulopoiesis, as recapitulated *in vitro* using human promyelocytic leukemia[9] (HL-60) cells, major alterations occur in the expression levels of two key nuclear envelope proteins: the integral nuclear membrane protein, lamin B receptor (LBR), is strongly upregulated, while there is a concurrent decrease in levels of lamin A, a key structural protein that forms a network underlying the inner nuclear membrane and imparts the nucleus with mechanical stability (11-13). Thus, while the unique shape of the neutrophil nucleus could facilitate the passage of these cells through narrow constrictions, we hypothesized that reduced levels of lamin A could enhance nuclear deformability and thereby facilitate the passage of cells through micron-scale constrictions.

To dissect the role of nuclear shape and nuclear envelope composition in the passage of cells through constrictions that mimic physiological gaps, we used all-trans-retinoic acid (ATRA)-stimulated HL-60 cells to recapitulate granulopoiesis; this *in vitro* system is widely used for structural and functional assays of white blood cells (14-16). We probed the ability of cells to transit through micron-scale constrictions and investigated the effects of both altered

nuclear shape and lamin A expression levels. Our results show that levels of lamin A have a predominant effect on the ability of cells to passage through narrow constrictions, whereas the altered shape of the neutrophil nucleus is not essential for rapid passage through micron-scale pores.

EXPERIMENTAL PROCEDURES

Cell culture – HL-60/S4 cells were maintained in RPMI-1640 media with L-Glutamine (Invitrogen), 10% fetal bovine serum (FBS), and 1% Pen/Strep (Gemini BioProducts, Calabasas, USA). We generated scrambled control cells to compare to HL-60/S4 cells with stable shRNA-mediated knockdown of LBR (LBR KD cells) (17). To induce differentiation into neutrophil-type cells, we added all-trans-retinoic acid (ATRA) at a final concentration of 5 μM to 1×10^5 cells/ml; ethanol was used as vehicle control. We probed nuclear shape and nuclear envelope composition at days 0, 3, and 5 after ATRA treatment; we performed functional assays of neutrophil-type cells at four days after ATRA treatment, when cells display characteristics of neutrophils (11,18).

Microfluidic deformation – Soft lithography was used to fabricate microfluidic channels in polydimethylsiloxane (PDMS, Sylgard 184 Silicone Elastomer, Dow Corning, USA) (19). Devices were bonded to #1.5-thickness coverglasses. We drove the flow of cells by applying 28 kPa (4 psi) of pressure to a tube of 2.5×10^6 cells/mL with 0.1% F127 (Pluoronic F-127, Invitrogen) to minimize surface adhesion (20). Images were acquired at 300 frames per second with a high-speed camera (Miro ex4, Vision Research, Wayne, USA) mounted on an inverted light microscope (Zeiss Observer) with 10×/0.25 Ph1 objective (A-Plan, Zeiss). The resulting image sequences were analyzed using a custom-written program (MATLAB) to extract the time for cell passage through the first constriction.

Retroviral transduction – We generated the stably modified lamin A overexpressing (LamA OE) cells from the parent HL-60/S4 cell line by retroviral transduction (21-23). We generated the stably modified lamin A overexpressing (LamA OE) cells from the parent HL-60/S4 cell line by retroviral transduction with the bicistronic vector (pRetroX-IRES-ZsGreen1, Clontech) for lamin A and the fluorophore reporter Zoanthus Green Fluorescent protein (ZsGreen1) with the 5' Moloney murine leukemia virus (MMLV) LTR as the promoter. Cloning of the wild-type Prelamin A into the bicistronic retroviral vector was performed as follows: the insert was generated by cutting pSVK3-Prelamin A(24) (kind gift from Howard J. Worman) with SmaI and SalI; this was ligated to the vector obtained from cutting pEGFP-C1 (Clontech) with Ecl136II and SalI resulting in a shuttle vector, which was subsequently digested with XmaI, blunt with Klenow, and then cut with BglII. The insert from the latter digestion was then ligated to the vector generated from cutting the pRetroX-IRES-ZsGreen1 with BamHI, blunt with Klenow, followed by BglII digestion. Transfection of the resultant pRetro-Prelamin A-IRES-ZsGreen 1 expression vector into the 293GPG retroviral packaging cell line (kind gift from Richard C. Mulligan) was performed using Lipofectin PLUS Reagent (Invitrogen) based on manufacturer's specifications and previous protocols with minor modifications (21-23). A ZsGreen1 retrovector without lamin A insert was used to generate the mock control cells. Viral supernatant was collected daily for 6 consecutive days, filtered through 0.45 μm pores, and stored at –20°C. Later, the viral sups collected per batch were thawed, pooled, and viral titer was determined by viral infection of mouse embryo fibroblasts.

Two rounds of viral transduction of HL-60/S4 cells were then performed using non-concentrated viral supernatant supplemented with 6-8 μg/ml Polybrene (Sigma-Aldrich) at a multiplicity of infection (MOI) of 25 to 50. Gene transfer efficiency was assayed five days after retroviral infection by flow cytometry probing ZsGreen1 levels; since ZsGreen1 and lamin A are derived from the same bicistronic mRNA transcript, we sorted individual cells based on ZsGreen1 levels into a subpopulation of cells with well-defined, elevated expression levels by fluorescence activated cell sorting (Aria II, BD Biosciences or MoFlo, Beckman Coulter) into calcium-free PBS buffer. The resulting subpopulation does not derive from a single clone, but is rather generated by the highest-expressing cells that may contain multiple insertions: the 5' LTR promoter is relatively weak, and we observe ~20- to 30-fold increase in lamin A levels in comparison to the mock controls.

Analysis of protein expression – Cell lysates were prepared from 5×10^6 cells using urea lysis buffer with final concentrations of 9 M urea, 10 mM Tris-HCl (pH 8), 10 μM EDTA, 500 μM phenylmethylsulfonyl fluoride, 20 μL beta-mercaptoethanol, and 1 μL/mL protease inhibitor cocktail (Sigma). All steps were performed at 4°C. Proteins were separated on a 4 – 12% Bis-Tris gel with 1x MOPS running buffer, then transferred onto activated transfer membranes, blocked, and labeled using horseradish peroxidase-conjugated antibodies (Biorad). We used protein standard (Invitrogen SeeBlue Plus2) for size calibration, and beta-tubulin as a loading control, since its levels remain constant throughout differentiation (11). Primary antibodies used for probing are described in SI Methods. Expression levels were quantified by optical density analysis using ImageJ (National Institutes of Health).

Cell surface marker analysis – To assay expression levels of CD11b, we used Fc receptor polyclonal human IgG (Sigma) as a blocking agent, and labeled 10^6 cells with Alexa Fluor 700 Mouse Anti-Human-CD11b (BD Pharmingen). We analyzed fluorescence levels by flow cytometry (LSRII, BD Biosciences).

Respiratory burst assay – We determined superoxide radical production of day 4/ATRA-treated cells using luminol-enhanced chemiluminescence (Diogenes reagent, National Diagnostics, Atlanta, USA) following stimulation by phorbol 12-myristate 13-acetate (PMA) (25,26), as per the manufacturer's instructions. Cells were activated by addition of PMA (stock solution 1 mg/ml DMSO, Sigma) to a final concentration of 11 μM; we recorded luminescence values after 30 min using a plate reader (Spectra Max M5).

Nuclear shape analysis – We incubated cells with Hoechst 33342 (1 μg/mL, Invitrogen) for 30 minutes at 37°C. We then placed the cells on a glass slide pretreated with poly-L-lysine (0.01% w/v in water) by centrifuging a 20 μL drop of cell suspension at 1,000 rpm for 5 sec. Images were acquired using a 20×/0.5 Ph2 objective (EC Plan Neofluar, Zeiss), DAPI filter set, and CCD camera (AxioCam MRm, Zeiss). Analysis of nuclear geometry was performed using ImageJ. Circularity for a nuclear cross-section is $4\pi A/P^2$, where A is the cross-sectional area and P is the perimeter.

Transwell migration assay – We used membranes with 3 and 8 μm pore sizes (Millipore) and FBS as chemoattractant (27,28). Day 4/ATRA-treated cells were resuspended to 5×10^6 cells/mL in RPMI without FBS. We placed media with and without FBS in the bottom well; cells in the top well, and then incubated the plate at 37°C, 5% CO_2 for 2 hrs. We then removed the membrane insert, labeled cells in the

bottom well with Hoechst, and imaged each well by microscopy using a 10×/0.25 Ph1 objective (A-Plan, Zeiss), CCD camera (AxioCam MRm, Zeiss), and DAPI filter set. We determined the number of cells per well using image analysis (Image J).

Two-dimensional migration assay – Glass-bottomed dishes (World Precision Instruments, Sarasota, USA) were coated with human fibronectin (10 µg/mL in HBSS without calcium and magnesium, Gemini Bioproducts, West Sacramento, USA). Cells were seeded onto the dishes, and images were acquired at one-minute intervals over three hours (5% CO_2, 37°C) using a Zeiss microscope outfitted with an automated stage (Applied Scientific Instruments, Eugene, USA), 10×/0.3 Ph objective (EC-Plan Neofluar, Zeiss), and CCD camera (AxioCam MRm, Zeiss); x-y positions of cells were extracted from the resultant movies (ImageJ), and trajectory analysis is performed using MATLAB.

RESULTS

Lobulated nuclear shape is not essential for cell transit – To probe the ability of neutrophil-type cells with round or lobulated nuclei to deform through narrow gaps, we designed a microfluidic device with precisely defined constrictions of 5 µm-width (Fig. 1 A); this width is less than the typical 7-10 µm diameter of HL-60 nuclei, such that nuclear deformation is required for a cell to passage through a pore (SI Fig.S1A). We forced the neutrophil-type cells (Day 4/ATRA-treated HL-60 cells) to transit through these micron-scale pores using pressure to drive a flow of cell suspension through the channels; we monitored the passage of cells as a function of time. When a cell arrives at a constriction, it is subjected to physical forces resulting from external stresses due to the pressure drop across the cell trapped in the constriction; these stresses cause the cell to deform and passage through the pore. Given the dimensions of a single pore, a pressure of 28 kPa corresponds to approximately µN-scale forces. The rate at which the cell deforms largely depends on the applied stress (driving pressure) as well as the global mechanical properties of the cell and nucleus (5,29-32) As individual cells deformed through the 5 µm constrictions of the microfluidic device, we imaged their passage using a high-speed camera (Fig. 1B, D). By automated image analysis, we determined the time required for the cell to passage through the first 5 µm constriction, which we define as its passage time. Given these millisecond timescales of cell passage at a driving pressure of 28 kPa, this microfluidic assay primarily probes the cell's passive mechanical behavior, as actin remodeling and protein expression changes occur on timescales of several minutes and more (33). While actin can contribute to the cortical stiffness of neutrophils (4-6), we confirmed that the actin makes little contribution to these measurements by treating a subset of neutrophil-type cells with cytochalasin D to disrupt actin polymerization; this treatment had no effect on passage times (data not shown), indicating that the deformability of the nucleus has a pivotal role in the passage of cells through micron-scale pores.

To assess the effect of hypolobulated or round-shaped nuclei on the passage of neutrophil-type cells through micron-scale constrictions, we used LBR KD cells as an *in vitro* system. In contrast to the control cells that exhibit strong upregulation of LBR during differentiation and develop lobulated nuclei, LBR KD cells show only trace levels of LBR expression and maintain round nuclei (17). Nevertheless, despite their round nuclei, LBR KD cells exhibited similar passage times compared to the scrambled control cells (Fig. 1B). These observations suggest that the multi-lobed shape of nuclei in mature neutrophils

provides no significant advantage in the time required for cells to deform through 5 μm constrictions.

Generating neutrophil-type cells with increased lamin A expression – Since the above experiments indicate that lobulated nuclear shape is not essential for neutrophil-type cell passage through narrow constrictions, we hypothesized that the unique molecular composition of the nuclear envelope in neutrophils could determine the ability of cells to deform. One possible origin may be the low levels of the key structural protein of the nucleus, lamin A; this protein is normally downregulated by over 90% in ATRA-stimulated HL-60 cells after four to five days of stimulation (Fig. 2B) (11,14). Given the essential role of lamin A in nuclear mechanical stability (12,13,30), we postulated that preventing lamin A downregulation could reduce nuclear deformability and impair cell passage through pores. Since the LBR KD neutrophil-type cells that have round nuclei have similar reduced lamin A expression levels as non- and mock-modified cells, this may also explain their unaltered passage times (17).

To test the effect of *increased* lamin A levels on cell passage through narrow constrictions, we generated a lamin A-overexpressing (LamA OE) HL-60 cell line by retroviral transduction. The resulting subpopulation of high-expressing cells exhibits lamin A levels that are about 20- to 30-fold higher than the mock-modified cells (SI Fig. S2A). While lamin A expression levels in the LamA OE cells are greater than those in non-modified HL-60 cells, they are comparable to physiological levels in other somatic cells such as mouse embryo fibroblast cells (SI Fig. S2B). To confirm that the ectopic lamin A is properly localized to the nuclear envelope, we conducted immunofluorescence and confocal imaging (SI Fig. S3).

Protein composition of LamA OE cells – To characterize how protein levels of the LamA OE cells change during granulopoiesis, we monitored expression levels of major structural proteins over the differentiation time-course: we induced the HL-60 cells to differentiate into neutrophil-type cells by ATRA treatment, collected cell lysates at days 0, 3, and 5 following ATRA treatment, and performed immunoblotting (Fig. 2A). As expected, non- and mock-modified cells displayed a strong upregulation of LBR during granulopoiesis with a concurrent decrease in lamin A levels (Fig. 2B,C), confirming previous observations (11). In contrast, LamA OE cells have increased levels of lamin A that further increased during granulopoiesis (Fig. 2B,C), possibly due to an ATRA-sensitive element in the ectopic promoter region. LamA OE cells showed elevated basal levels of LBR compared to the mock controls, with a similar ~4-fold increase in LBR levels during granulocytic differentiation. We also probe levels of other structural proteins that could contribute to cell deformability (4-6): during differentiation in both the mock-modified and LamA OE cells, actin levels showed minor variations, and other structural nuclear proteins including lamin B1 and B2, showed a decrease in expression levels (Fig. 2) (34). While we cannot exclude the possible contribution of lamin B1 and B2 downregulation to altered cellular mechanical properties, we anticipate that the observed changes in lamin B1/B2 levels would have little effect on nuclear mechanical properties in comparison to the lamin A upregulation: lamins A/C have a predominant role in nuclear shape stability and stiffness (12,13,30), whereas lamin B1 does not have any significant effect on nuclear mechanical stability (13).

Genetically modified cells display characteristics of neutrophils – To test whether the genetically modified HL-60

cells still undergo normal granulopoiesis, we assayed essential functional, biochemical, and proteomic characteristics that define neutrophils. One metric to assess the differentiation of HL-60 cells into neutrophil-type cells is to measure cell density following ATRA stimulation; decreased proliferation rates are an indicator of successful differentiation as cells exit the cell cycle to commit to their differentiation into neutrophils (35). Both LBR KD and LamA OE cells showed a similar progressive decrease in proliferation rates over the days following ATRA treatment as compared to the scrambled and mock controls (SI Fig. S4). As a more direct assay of differentiation into neutrophil-type cells, we measured expression levels of the cell surface marker, CD11b, a subunit of a heterodimeric adhesion glycoprotein, which is widely used as a marker for neutrophils (36). After four days of ATRA treatment, CD11b levels were increased for all cell types compared to the non-differentiated HL-60 cells and vehicle-treated controls (SI Fig. S5). These results confirmed that the HL-60 cells are differentiating into neutrophil-type cells. Importantly, we observed that all cell lines show significant increase in CD11b levels following ATRA stimulation, with levels varying slightly between cell lines (Fig. 2D); this demonstrates that the changes in nuclear envelope composition do not markedly affect differentiation efficiency.

Another hallmark of neutrophil cells is their respiratory burst response upon exposure to phagocytotic stimuli, such as yeast or bacteria. To probe this functional characteristic of the modified neutrophil-type cells, we stimulated cells with phorbol myristate acetate and measured subsequent superoxide production (Fig. 2E). LBR KD cells showed similar response compared to the scrambled controls. LamA OE cells exhibited a small yet statistically significant 15% reduction in superoxide production compared to the mock controls. Overall, these experiments suggest that the functional and biochemical characteristics of the genetically modified neutrophil-type cells are generally maintained despite their altered nuclear envelope composition.

Lamin A expression alters nuclear lobulations during granulopoiesis – A key hallmark of granulopoiesis is the transition from round to multi-lobed nuclear shape, which is observed in HL-60 cells after three to five days following ATRA-treatment (11,18). To investigate the effect of altered nuclear envelope composition on this shape transition, we imaged Hoechst-stained nuclei by fluorescence microscopy over the differentiation time-course. To quantify changes in nuclear shape, we analyzed the circularity of nuclei, defined as $4\pi A/P^2$, where A is the cross-sectional area and P is the perimeter of an individual nuclear cross-section. For a perfect circle, the circularity value equals one; lower values reflect deviations from a circular shape. In the undifferentiated state, all cell lines have nuclei with predominantly circular shape and similarly high circularity values, representative of round nuclei (Fig. 3A, B, C).

After three days of ATRA-treatment, the non-modified, mock, and scrambled control cells exhibited nuclei with large invaginations; circularity values correspondingly showed a lower median and greater variability, reflecting these irregular nuclear shapes. By contrast, LBR KD cells retained their round shape, as reflected by the higher circularity values, even after five days of ATRA treatment (Fig. 3A) (17). The nuclei of LamA OE cells showed some morphological changes but failed to develop the characteristic lobulations seen in the non-modified and mock control cells (Fig. 3A, SI Fig. S3); the lack of severe lobulation that is typical for normal neutrophil cells

illustrates that downregulation of lamin A expression during neutrophil differentiation could also be required for the lobulated nuclear shape of mature neutrophils.

Increased lamin A expression delays cell passage through pores – Lamin A is a crucial modulator of nuclear deformability (13,30,37). To probe the effects of increased lamin A levels on the ability of cells to deform through physiological gaps, we measured the passage time of LamA OE neutrophil-type cells and mock controls when forced through the 5 μm-constrictions of our microfluidic device (Fig. 1A,D). The LamA OE neutrophil-type cells exhibited a three-fold increase in median passage time as compared to the mock controls (Fig. 1E); these results indicate that increased density of lamin protein at the nuclear envelope may impair the ability of LamA OE neutrophil-type cells to passage through the 5 μm constrictions. Taken together, our results show that lamin A levels have an important effect on the ability of cells to passage through 5 μm constrictions: physiological *downregulation* of lamin A following ATRA-induced differentiation of HL-60 cells results in *faster passage* through the micron-scale constrictions, whereas ectopically *increased expression* of lamin A results in *slower passage* of LamA OE-neutrophils through the 5 μm constrictions.

Active migration through pores is impaired in LamA OE cells – The results of our microfluidic experiments illustrate that altered expression of lamin A can substantially alter the passive deformability of cells. Yet a critical function of neutrophils is their ability to *actively* migrate through narrow constrictions. To test migration efficiency, we used a transwell migration assay to probe the ability of cells to migrate through 3 and 8 μm pores: we monitored the number of cells that migrate through the pores after two hours, and determined the migration efficiency relative to the respective control cells. As seen in the passive deformation results obtained by microfluidic assays, the LBR KD cells exhibited similar migration efficiency as the scrambled control cells (Fig. 4A, B), further substantiating that neutrophil-type cells with round nuclei can exhibit equivalent passage efficiency through micron-scale pores. By contrast, the LamA OE cells showed a marked reduction in migration through 3 μm pores (Fig. 4D, E). The impaired migration was less severe in the experiments with 8 μm pores (Fig. 4D, E); since deformation through 8 μm pores requires smaller deformations of nuclei, these results are consistent with our observations that nuclear deformation rate-limits the passage of cells through micron-scale constrictions.

To address the possibility that a general migration defect underlies the impaired transwell migration efficiency of the LamA OE cells, we performed two dimensional migration assays; cells exhibited velocities from 2 to 5 μm/min, consistent with previous observations of neutrophil migration (38). The LBR KD cells showed a slightly increased velocity compared to the scrambled-control cells (Fig. 4C). Importantly, LamA OE cells exhibited similar migration velocities as the mock-control cells (Fig. 4F), indicating that the observed differences in the transwell assay cannot be attributed to general defects in their migration. Taken together, our experiments indicate that the density of lamin A at the nuclear envelope is crucial in facilitating passage of cells through micron-scale constrictions.

DISCUSSION

It has long been speculated that the lobulated shape of the neutrophil nucleus is ‘a special adaptation for passing through vessel walls’ (8). Yet here we show that nuclear shape alone does not always determine the timescale for neutrophil deformation through micron-scale pores:

neutrophil-type cells with round nuclei resulting from LBR knockdown (17) show unaltered passage efficiency through pores down to 3 μm, as probed using both passive deformation through 5 μm microfluidic constrictions, as well as active migration through 3 and 8 μm porous membranes.

These LBR KD cells also provide an *in vitro* model for Pelger-Huët anomaly (PHA): the nuclei from neutrophils of these individuals are round or bi-lobulated (36,37) due to a complete or partial lack of functional LBR. The extent to which the altered nuclear shape of PHA neutrophils affects their ability to passage through micron-scale constrictions has been inconclusive (26,39-41). Some previous studies of these neutrophils discovered altered migration; however, these primary neutrophils also exhibited bi-lobular nuclei, and differences in migratory ability could result from other phenotypic differences. Here we used LBR KD cells as an *in vitro* system to specifically investigate the effect of the hypolobulated nucleus on cell passage through micron-scale constrictions. Despite the round shape of LBR KD nuclei, which could sterically hinder the passage of nuclei through constrictions, these cells exhibited similar passage efficiencies through micron-scale constrictions as compared to the scrambled control cells with multi-lobed nuclei (Fig.1).

While LBR KD neutrophil-type cells have an atypical round nuclear shape, they have similarly low levels of lamin A as the non-modified controls (17). Here, we show that lamin A expression levels, rather than the shape of the cell nucleus, can be a major determinant of the timescale of cell passage through micron-scale gaps (Fig. 5). By contrast, non-mechanical functions of these cells are not substantially affected by changes in nuclear envelope composition. While other types of white blood cells with ovoid-shaped nuclei, such as macrophages, also undergo transendothelial migration, their deformations occur on a slower timescale compared to neutrophils (31). Indeed, monocyte/macrophage-differentiated HL-60 cells also show increased levels of lamin A/C expression relative to neutrophil-type cells (34).

If irregular nuclear shape is not essential for the deformability of neutrophil cells, then why do their nuclei exhibit this distinct shape? One possibility is that the multi-lobed nucleus could simply result from the marked changes in nuclear envelope protein composition. Indeed, lamin A levels impact the mechanical stability of the nuclear envelope, while ectopic overexpression of LBR can increase nuclear membrane surface area (42,43) (Fig. 5). Alternatively, the unusual multi-lobed nuclear shape may facilitate other neutrophil functions, such as phagocytosis, the formation of neutrophil extracellular traps (NETs), or migration through even smaller < 1 μm constrictions of the endothelium, either between or through cells (44).

Here we have used HL-60 cells, which are a well-established *in vitro* model system to study white blood cell lineages: for example, the resulting neutrophil-type cells show similar structural and functional characteristics as primary neutrophils (14-16). HL-60 cells also exhibit similar mechanical properties: recent measurements of cell compliance using an optical stretcher confirmed that *in vitro* differentiation of HL-60 cells into neutrophil-type cells recapitulates the 3- to 6-fold increase in cell deformability observed in primary neutrophils and their CD34+ precursor cells (31). A direct comparison of the absolute passage times through micron-sized constriction between primary neutrophils and HL-60-derived neutrophil-type cells is complicated by the fact that HL-60 cells are typically larger than primary neutrophils (~12 μm *vs*. 7–8 μm median diameter,

respectively) and exhibit substantially larger transit times through microfluidic constriction channels (29). Consequently, we have focused our study on HL-60 cells and vary protein levels within the same cell type; this has enabled us to clearly illustrate the importance of nuclear envelope composition, particularly the levels of lamins A/C, on the ability of cells to pass through narrow constrictions during perfusion and migration.

It is intriguing to speculate that changes in levels of lamin A expression may have implications for cellular deformability in a variety of physiological processes and diseases (45). For example, certain types of cancer cells have reduced levels of lamin A expression compared to their non-malignant progenitors (46,47). Akin to neutrophils, large deformations of cancer cells and their nuclei are required during deformation through micron-scale constrictions (48) in extravasation and metastasis. Ultimately, a deeper knowledge of the molecular basis of cellular and nuclear deformability will provide unique insights into the mechanical aspects of cell biology and possibly new therapeutic approaches.

REFERENCES

1. Doerschuk, C. M., Beyers, N., Coxson, H. O., Wiggs, B., and Hogg, J. C. (1993) *J Appl Physiol* **74**, 3040-3045
2. Worthen, G. S., Schwab, B., 3rd, Elson, E. L., and Downey, G. P. (1989) *Science* **245**, 183-186
3. Downey, G. P., Worthen, G. S., Henson, P. M., and Hyde, D. M. (1993) *Am Rev Respir Dis* **147**, 168-176
4. Tsai, M. A., Waugh, R. E., and Keng, P. C. (1998) *Biophysical Journal* **74**, 3282-3291
5. Tsai, M. A., Frank, R. S., and Waugh, R. E. (1994) *Biophys J* **66**, 2166-2172
6. Ting-Beall, H. P., Lee, A. S., and Hochmuth, R. M. (1995) *Annals Biomed Eng* **23**, 666-671
7. Lautenschlager, F., Paschke, S., Schinkinger, S., Bruel, A., Beil, M., and Guck, J. (2009) *Proc Natl Acad Sci U S A* **106**, 15696-15701
8. Hirsch, J. G. (1959) *Bacteriol Rev.* **23**, 48-60
9. Erzurum, S. C., Kus, M. L., Bohse, C., Elson, E. L., and Worthen, G. S. (1991) *Am J Respir Cell Mol Biol* **5**, 230-241
10. Downey, G. P., Doherty, D. E., Schwab, B., 3rd, Elson, E. L., Henson, P. M., and Worthen, G. S. (1990) *J Appl Physiol* **69**, 1767-1778
11. Olins, A. L., Herrmann, H., Lichter, P., and Olins, D. E. (2000) *Exp Cell Res* **254**, 130-142
12. Lammerding, J., Schulze, P. C., Takahashi, T., Kozlov, S., Sullivan, T., Kamm, R. D., Stewart, C. L., and Lee, R. T. (2004) *J Clin Invest* **113**, 370-378
13. Lammerding, J., Fong, L. G., Ji, J. Y., Reue, K., Stewart, C. L., Young, S. G., and Lee, R. T. (2006) *J Biol Chem* **281**, 25768-25780
14. Olins, A. L., Buendia, B., Herrmann, H., Lichter, P., and Olins, D. E. (1998) *Exp Cell Res* **245**, 91-104
15. Collins, S. J. (1987) *Blood* **70**, 1233-1244
16. Gallagher, R., Collins, S., Trujillo, J., McCredie, K., Ahearn, M., Tsai, S., Metzgar, R., Aulakh, G., Ting, R., Ruscetti, F., and Gallo, R. (1979) *Blood* **54**, 713-733

17. Olins, A. L., Ernst, A., Zwerger, M., Herrmann, H., and Olins, D. E. (2010) *Nucleus* **1**, 1-7
18. Meyer, P. A., and Kleinschnitz, C. (1990) *Environ Health Perspect* **88**, 179-182
19. Duffy, D. C., McDonald, J. C., Schueller, O. J. A., and Whitesides, G. M. (1998) *Anal. Chem.* **70**, 4974-4984
20. Gomez-Sjoberg, R., Leyrat, A. A., Pirone, D. M., Chen, C. S., and Quake, S. R. (2007) *Anal Chem* **79**, 8557-8563
21. Ory, D. S., Neugeboren, B. A., and Mulligan, R. C. (1996) *Proc Natl Acad Sci U S A* **93**, 11400-11406
22. Jaalouk, D. E., Lejeune, L., Couture, C., and Galipeau, J. (2006) *Virol J* **3**, 97
23. Spitzer, D., Wu, X., Ma, X., Xu, L., Ponder, K. P., and Atkinson, J. P. (2006) *J Immunol* **177**, 4953-4956
24. Boguslavsky, R. L., Stewart, C. L., and Worman, H. J. (2006) *Hum Mol Genet* **15**, 653-663
25. Teufelhofer, O., Weiss, R. M., Parzefall, W., Schulte-Hermann, R., Micksche, M., Berger, W., and Elbling, L. (2003) *Toxicol Sci* **76**, 376-383
26. Gaines, P., Tien, C. W., Olins, A. L., Olins, D. E., Shultz, L. D., Carney, L., and Berliner, N. (2008) *Exp Hematol* **36**, 965-976
27. Auguste, K. I., Jin, S., Uchida, K., Yan, D., Manley, G. T., Papadopoulos, M. C., and Verkman, A. S. (2007) *FASEB J* **21**, 108-116
28. Muinonen-Martin, A. J., Veltman, D. M., Kalna, G., and Insall, R. H. (2010) *PLoS One* **5**, e15309
29. Rosenbluth, M. J., Lam, W. A., and Fletcher, D. A. (2008) *Lab Chip* **8**, 1062-1070
30. Pajerowski, J. D., Dahl, K. N., Zhong, F. L., Sammak, P. J., and Discher, D. E. (2007) *Proc Natl Acad Sci U S A* **104**, 15619-15624
31. Ekpenyong, A. E., Whyte, G., Chalut, K., Pagliara, S., Lautenschlager, F., Fiddler, C., Paschke, S., Keyser, U. F., Chilvers, E. R., and Guck, J. (2012) *PLoS One* **7**, e45237
32. Bathe, M., Shirai, A., Doerschuk, C. M., and Kamm, R. D. (2002) *Biophys J* **83**, 1917-1933
33. Cano, M. L., Lauffenburger, D. A., and Zigmond, S. H. (1991) *J Cell Biol* **115**, 677-687
34. Olins, A. L., Herrmann, H., Lichter, P., Kratzmeier, M., Doenecke, D., and Olins, D. E. (2001) *Exp Cell Res* **268**, 115-127
35. Fleck, R. A., Athwal, H., Bygraves, J. A., Hockley, D. J., Feavers, I. M., and Stacey, G. N. (2003) *In Vitro Cell Dev Biol Anim* **39**, 235-242
36. Gaines, P., and Berliner, N. (2005) *Curr Protoc Immunol* **Chapter 22**, Unit 22F 25
37. Rowat, A. C., Lammerding, J., Herrmann, H., and Aebi, U. (2008) *BioEssays* **30**, 226-236
38. Gonzalez, A. L., El-Bjeirami, W., West, J. L., McIntire, L. V., and C.W., S. (2007) *J Leukocyte Biol* **81**, 686-695
39. Park, B. H., Dolen, J., and Snyder, B. (1977) *Proc Soc Exp Biol Med* **155**, 51-54
40. Repo, H., Vuopio, P., Leirisalo, M., Jansson, S. E., and Kosunen, T. U. (1979) *Clin Exp Immunol* **36**, 326-333
41. Matsumoto, T., Harada, Y., Yamaguchi, K., Matsuzaki, H., Sanada, I., Yoshimura, T., Honda, M., and Tanaka, R. (1984) *Acta Haematol* **72**, 264-273
42. Ellenberg, J., Siggia, E. D., Moreira, J. E., Smith, C. L., Presley, J. F., Worman, H. J., and Lippincott-Schwartz, J. (1997) *J Cell Biol* **138**, 1193-1206

43. Ma, Y., Cai, S., Lv, Q., Jiang, Q., Zhang, Q., Sodmergen, Zhai, Z., and Zhang, C. (2007) *J Cell Sci* **120**, 520-530
44. Feng, D., Nagy, J. A., Pyne, K., Dvorak, H. F., and Dvorak, A. M. (1998) *J Exp Med* **187**, 903-915
45. Campbell, M. S., Lovell, M. A., and Gorbsky, G. J. (1995) *J Leukoc Biol* **58**, 659-666
46. de Las Heras, J. I., Batrakou, D. G., and Schirmer, E. C. (2012) *Semin Cancer Biol*
47. Zink, D., Fischer, A. H., and Nickerson, J. A. (2004) *Nat Rev Cancer* **4**, 677-687
48. Fu, Y., Chin, L. K., Bourouina, T., Liu, A. Q., and Vandongen, A. M. (2012) *Lab Chip* **12**, 3774-3778

Acknowledgements – We acknowledge the Center for Nanoscale Systems, Harvard University, for access to the profilometer, and Bino Varghese for advice on data analysis protocols. Cell sorting was performed by Brian Tilton, Bauer Center at Harvard University, and Jeff Calimlim in the UCLA Jonsson Comprehensive Cancer Center (JCCC) and Center for AIDS Research Flow Cytometry Core Facility.

FOOTNOTES

* This work was supported by a Cross-Disciplinary Fellow of the International Human Frontiers Science Program (HFSP) to ACR and National Institutes of Health awards [R01 NS059348 and R01 HL082792] and the Department of Defense Breast Cancer Idea Award [BC102152] to JL. WLU and IAE acknowledge funding from NSERC, and DEJ acknowledges support by the American Heart Association Fellowship (AHA Award 09POST2320042). We also acknowledge HFSP Grant No. RGP0004/2005-C102, the NSF Contract Nos. DMR-1006546 and DBI-649865, and the Harvard MRSEC Contract No. DMR-0820484. The UCLA Jonsson Comprehensive Cancer Center (JCCC) and Center for AIDS Research Flow Cytometry Core Facility is supported by National Institutes of Health awards CA-16042 and AI-28697, and by the JCCC, the UCLA AIDS Institute, the David Geffen School of Medicine at UCLA, and the UCLA Chancellor's Office.

[1]To whom correspondence can be addressed: Amy C. Rowat, Department of Integrative Biology & Physiology, University of California, Los Angeles, 610 Charles E. Young Drive South, Los Angeles, CA 90095; email: rowat@ucla.edu
[2]Department of Medicine, Brigham and Women's Hospital/Harvard Medical School, 65 Landsdowne St, Cambridge, MA 02139
[3]Current Address: Department of Biology, American University of Beirut, Lebanon
[4]Current Address: Department of Biochemistry, University of Zurich, Switzerland
[5]Department of Physics and School of Engineering and Applied Sciences, Harvard University, Cambridge, MA 02138
[6]Department of Pharmaceutical Sciences, College of Pharmacy, University of New England, Portland, ME 04103
[7]Division of Molecular Genetics, German Cancer Research Center, D-69120 Heidelberg, Germany
[8]Weill Institute for Cell and Molecular Biology, Department of Biomedical Engineering, Cornell University, 235 Weill Hall, Ithaca, NY 14853

[9]The abbreviations used are: LamA OE – lamin A overexpressing, LBR – lamin B receptor; LBR KD – LBR knockdown, HL-60 – human promyelocytic leukemia, ATRA – trans-retinoic acid, LTR – Long terminal repeat

FIGURE LEGENDS

FIGURE 1. Ectopic expression of lamin A increases passage time through microfluidic constriction channels. A. Schematic overview of the microfluidic device and close-up of the 5 μm constrictions. Pressurizing the reservoir drives the cell suspension through the inlet, and cells passage through the channels with 5 μm constrictions, as shown in the inset. Scale, 20 μm. **B.** Time-sequence images of day 4/ATRA treated cells passaging through 5 μm-constrictions. **C.** LBR KD cells have similar passage times as the scrambled controls, despite the round shape of their nucleus that has been speculated to sterically hinder the passage of cells through narrow pores. **D, E.** LamA OE cells take longer to passage the constrictions than mock-control cells. In all boxplots, the white bar denotes the population median, boxes are the 25th and 75th percentiles, and lines show the 10th and 90th percentiles. n.s., $P > 0.05$ for LBR KD versus scrambled control; ***, $P < 0.001$ for LamA OE versus mock control. $N > 300$ cells for each cell type.

FIGURE 2. Genetically modified HL-60 cells show typical characteristics of neutrophils after ATRA stimulation. A. Representative immunoblots for lamins A/C, B1, B2, and LBR with beta-tubulin as loading control. Cell lysates are collected from LamA OE and mock control cells at days 0, 3, and 5 after ATRA stimulation. **B, C.** Quantitative analysis of lamin A and LBR protein levels normalized first to beta-tubulin and then to day 0 for each protein in each cell line. Error bars represent standard error of the mean of 3 to 5 independent experiments; where not visible, they are smaller than the symbols. Based on immunoblot analysis, baseline levels of lamin A are estimated to be ~20 to 30× greater in the LamA OE cells compared to the mock control cells (SI Fig.S2); for this reason, two separate axes are plotted for each cell line. **D.** Expression levels of the cell surface antigen, CD11b, a hallmark of neutrophils, increase during differentiation for all cell lines. Left, representative histograms of data from a single flow cytometry experiment showing the distribution of CD11b expression levels at day 4 after ATRA stimulation. Right, graphs showing median values of CD11b after ATRA treatment with the values for each cell line normalized to day 0 for each independent experiment. Error bars represent standard error of the mean over three independent experiments. **E.** Respiratory burst assay that probes superoxide production using a luminescence assay 30 min after stimulation by phorbol myristate acetate, indicating that all cells show normal functional characteristics of neutrophils. Luminescence values are relative to the mock and scrambled control for the left and right panels, respectively. Data represent the average of three independent experiments; error bars represent the standard error of the mean. n.s., $P > 0.05$ for LBR KD versus scrambled control; *, $P < 0.05$ for LamA OE versus mock control.

FIGURE 3. Nuclear shape transition during granulopoeisis requires lamin A downregulation and LBR upregulation. A. Fluorescent images of Hoechst-stained nuclei acquired at day 0 and day 5 after ATRA treatment. All images are acquired at the same magnification. Scale, 5 μm. **B.** To quantitatively describe nuclear shape, the circularity of the nucleus is defined as: $4\pi A/P^2$. Histograms show the distribution for each cell type at days 0 and 5 after ATRA treatment. **C.** Boxplots show the circularity of nuclei at days 0, 3, and 5 after ATRA

treatment. The white bar denotes the population median, boxes are the 25th and 75th percentiles, and lines show the 10th and 90th percentiles. To evaluate statistical significance, we compare the medians of at least 3 independent experiments for each cell type. Day 0, non-modified to scrambled control. N.s., $P > 0.05$; *, $P < 0.05$. Nuclei from over 300 individual cells are analyzed for each cell type.

FIGURE 4. Impaired migration of LamA OE cells through narrow constrictions. To probe the active migration of cells through micron-scale pores, we use a transwell migration assay. **A, D.** Representative images from a single experiment showing Hoechst-stained nuclei of cells that have passed through 3 μm or 8 μm pores. Scale, 100 μm **B, E.** Migration efficiency is defined as the number of cells that passaged through the porous membrane relative to the corresponding scrambled or mock control. Bars represent averages from at least three independent experiments; error bars represent standard error of the mean. ***, $P < 0.001$ for LamA OE versus mock control. **C, F.** 2D migration experiments are performed by tracking the position of individual cells at one-minute intervals over three hours. Traces of three representative cells for each cell type show the total distance traveled and the directionality of movement over the three-hour time-lapse experiment. Axes are 150 μm with 50 μm increments. Migration speed over the entire trajectory is computed from the individual traces of over 50 cells for each cell type. Mean values for each LBR KD and LamA OE cells are normalized to their respective controls. N.s., $P > 0.05$; *, $P < 0.05$; ***, $P < 0.001$. Absolute velocities of cells are: LBR KD, 4.4 – 5.1 μm/min; scrambled control, 3.5 – 4.2 μm/min; LamA OE, 2.2 – 4.7 μm/min; mock control, 2.8 – 4.8 μm/min.

FIGURE 5. Lamin A levels, rather than nuclear shape, is a primary determinant of the efficiency of cell passage through narrow constrictions. Schematic illustration summarizing the effects of nuclear shape and lamin A expression levels on the ability of cells to deform through narrow constrictions. The ratio of LamA to LBR expression levels is estimated from immunoblots. Non-differentiated (non- or mock modified) HL-60 cells, as well as the LBR KD neutrophil-type cells, exhibit efficient passage, despite their round nuclear shape. By contrast, lamin A overexpression results in impaired passage, both through the constricted 5 μm channels of a microfluidic device, as well as the 3 μm and 8 μm pores of the transwell migration assay. Non-differentiated LamA OE cells with more circular nuclei and lower levels of LBR require even longer time to passage through narrow constrictions.

FIGURE 1.

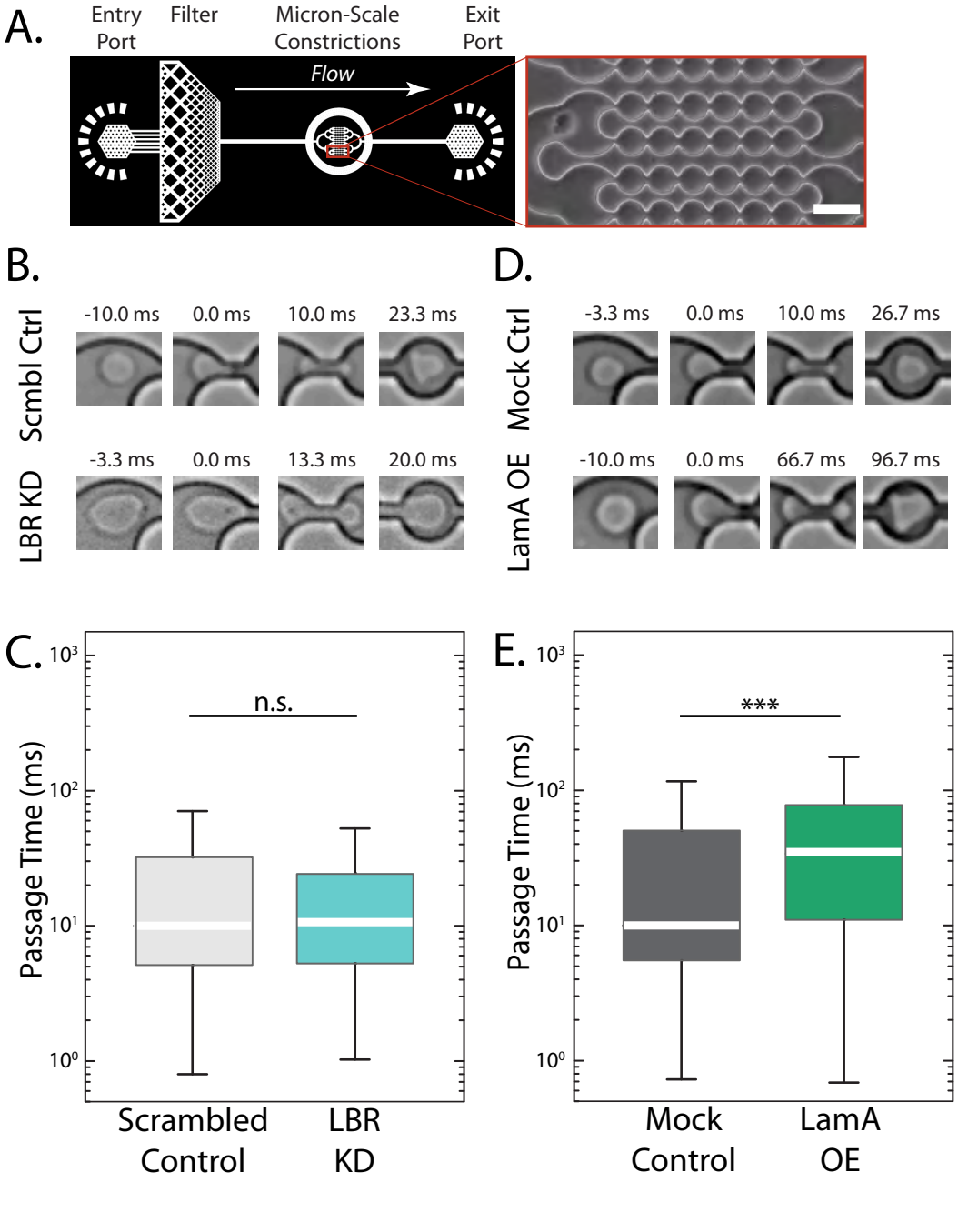

FIGURE 2.

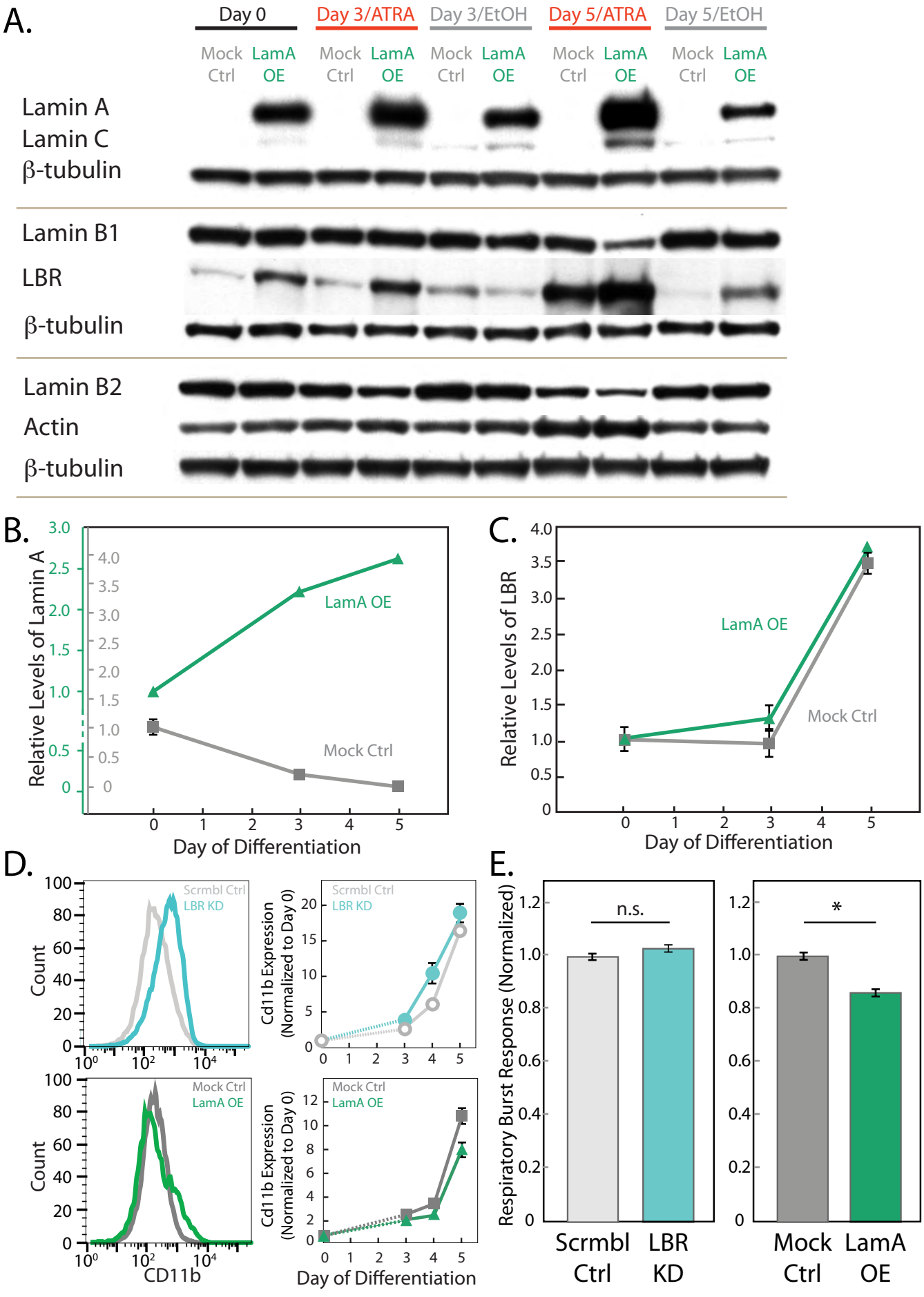

FIGURE 3.

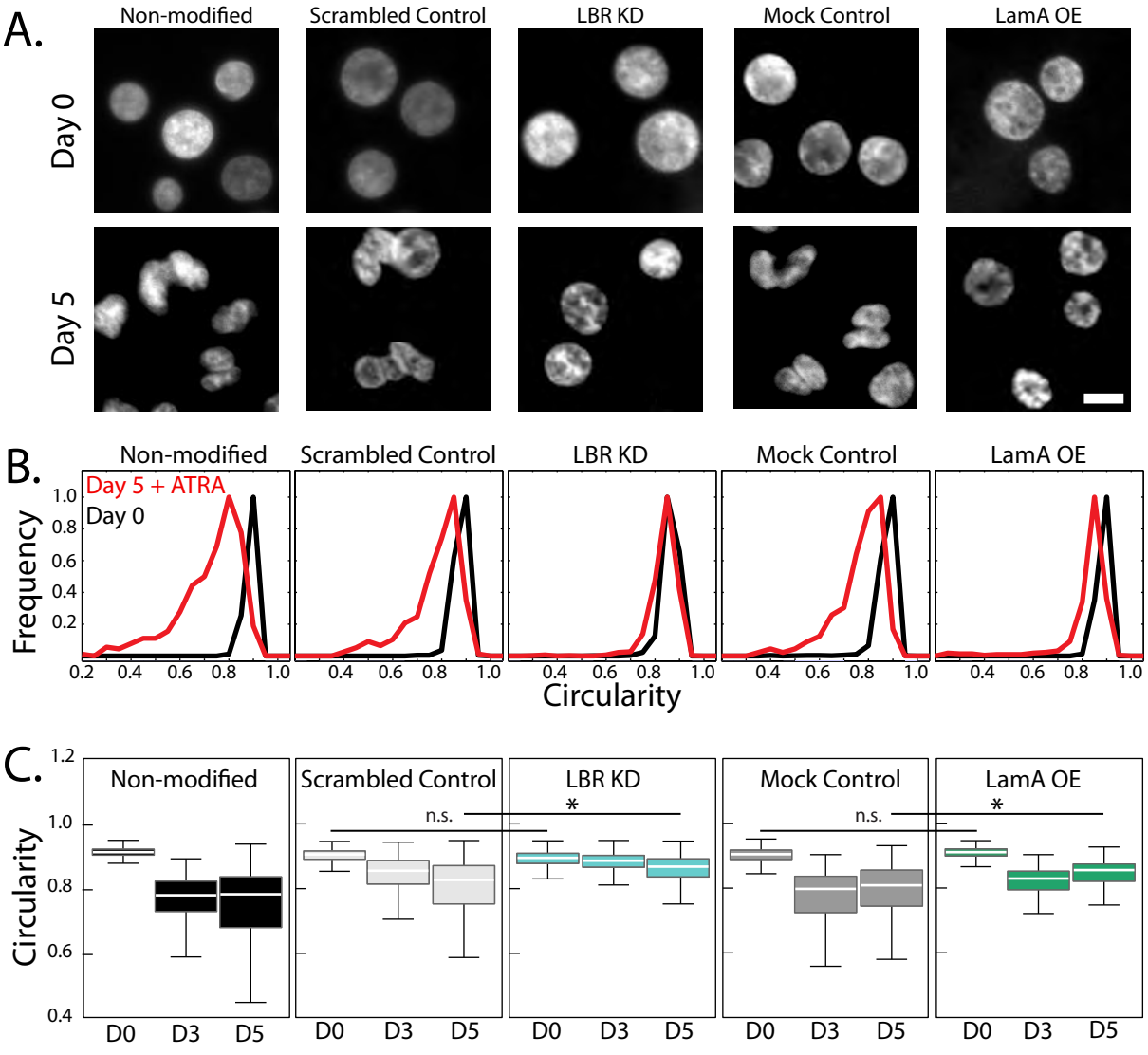

FIGURE 4.

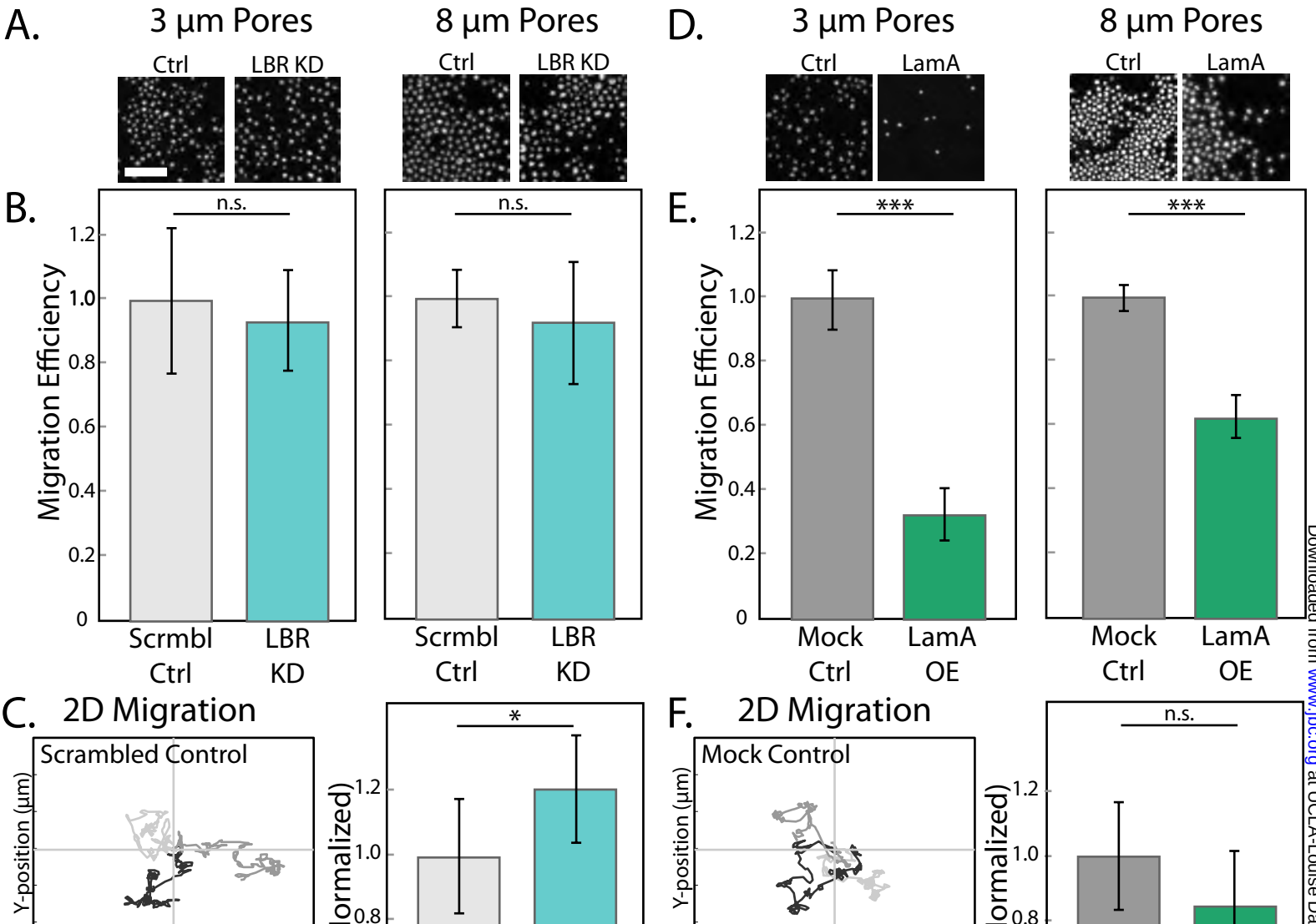

FIGURE 5.